Dielectric properties of polyamide-4,6

P. A. M. Steeman* and F. H. J. Maurer
DSM Research BV, PO Box 18, 6160 MD Geleen, The Netherlands
(Received 5 August 1991; revised 14 November 1991; accepted 13 January 1992)

The dielectric properties of polyamide-4,6 were examined as functions of frequency, temperature and moisture content. The dielectric spectra were compared with the results of dynamic mechanical measurements in torsion at 0.2153 Hz, as a function of temperature, and with the dynamic dielectric properties of commercial polyamide-6,6. Three relaxation processes are observed in polyamide-4,6, which are related to either local or collective molecular mechanisms of motion, similar to the relaxation processes observed in other polyamides. At temperatures above the glass transition temperature, ionic conductivity is observed, which, due to the semicrystalline structure of the material, gives rise to a strong Maxwell–Wagner–Sillars (MWS) polarization. With increasing temperature, the conductivity increases sharply, eventually causing electrode polarization, and thus obscuring the dielectric effects in the material. All loss processes shift to lower temperatures with increasing water content. The activation energies of the secondary relaxations decrease with increasing water uptake, while the β and α relaxations are enhanced in magnitude.

(Keywords: polyamide-4,6; Stanyl®; dielectric properties; dynamic mechanical properties; polyamide-6,6; water content; relaxation mechanisms)

INTRODUCTION

The dielectric properties of most polyamides have been examined by several authors. Detailed information and a review of existing literature can be found in McCrum *et al.*[1] and Hedvig[2]. In general, three polarization mechanisms related to molecular mechanisms of motion are observed. At lower temperatures (between -150 and -100°C) a weak polarization mechanism is found, which is thought to be due to the local motion of chain segments, mainly CH_2 segments, located between the interchain hydrogen bonds. Near -50°C a polarization mechanism is observed, which is related to a mechanism of motion (rotation) of the amide bonds together with water molecules that are bonded to them. At higher temperatures (40–70°C, depending on the type of polyamide) a strong relaxation is found, which corresponds to the glass–rubber transition of the amorphous phase. Above this transition temperature the materials become electrically conductive and show a sharp increase in dielectric constant[3,4], which is thought to be due to an interfacial, or Maxwell–Wagner–Sillars (MWS), polarization process as a result of trapping of free charge carriers at boundaries between crystalline and amorphous regions. Space-charge effects[5] as detected by the thermally stimulated discharge (t.s.d.c.) technique are related to this MWS polarization mechanism.

Recently polyamide-4,6 was introduced as a commercial product by DSM under the tradename Stanyl®. Because of the high number of amide groups per unit length of chain compared with other polyamides and the highly symmetrical chain structure, a high crystallization rate, high crystallinity and a high melting point of 295°C are obtained[6]. This leads to much better high-temperature physical properties, which make the material more suitable for modern electrical applications. Since no dielectric data are available for this material in the open literature, we report on its dielectric properties as a function of temperature, frequency and water content. The results are compared with dynamic mechanical measurements in torsion and with the dielectric properties of commercial polyamide-6,6.

EXPERIMENTAL

Materials

Polyamide-4,6 is an aliphatic polyamide prepared by polycondensation of 1,4-diaminobutane and adipic acid[7]. The material investigated in this work is the medium-molar-mass ($M_w = (4–4.5) \times 10^4$ g mol^{-1}, density = 1180 kg m^{-3}) grade Stanyl TE300, stabilized with a set of additives selected for use in electronic applications. No effects of these additives on the dielectric and mechanical properties of the material were detected. Samples, with dimensions of $40 \times 40 \times 1$ mm^3, were cut from injection-moulded plates (melt temperature 320°C, mould temperature 120°C).

The dielectric properties were measured on carefully dried samples and on samples that were equilibrated in 31% and 51% relative humidity environments at room temperature. The latter samples showed an equilibrium relative mass gain due to water uptake of 2.4 wt% and 4.3 wt%, respectively. In this paper we will call these samples the 2 wt% and 4 wt% samples, respectively. Since water desorbs from the wet samples during the measurements at elevated temperatures, the measurements on the wet samples become less well defined at higher temperatures. However, since the material is clamped between the plane plates of a capacitor, water desorption is strongly hindered.

*To whom correspondence should be addressed

0032-3861/92/204236-06
© 1992 Butterworth-Heinemann Ltd.

The polyamide-6,6 sample was injection moulded from a commercially available polyamide-6,6 (Maranyl A146® manufactured by ICI), with a density of 1140 kg m^{-3}.

Techniques

The dielectric measurements at low frequencies were performed with a dielectric spectrometer based on a Schlumberger type 1250 frequency response analyser (FRA), interfaced to the measurement capacitor by a custom-made dielectric feedback electrometer (built at TNO, the Dutch Organization for Applied Scientific Research). The response analyser applied a sinusoidal voltage with a frequency of between 100 mHz and 10 kHz and an amplitude of 10 V_{eff} to one plate of a parallel-plate sample capacitor. The other plate of the capacitor was virtually grounded by the electrometer, which measures the cell current and converts it to a voltage signal. Using capacitive detection, a very good signal-to-noise ratio was obtained over the full frequency range. The FRA measured the phase and amplitude relations between the applied generator signal and the converted sample current. High-frequency measurements were performed using a Hewlett–Packard type 4275A multifrequency LCR meter with a frequency range from 10 kHz to 10 MHz.

A gold electrode was sputtered on both surfaces of the sample using a Balzers sputter coater in order to assure good electrical contact between the sample and the gold-plated plates of the sample capacitor.

The sample capacitor was placed in a custom-made oven system (also TNO), which could be cooled and heated with a flow of dried nitrogen gas to temperatures between −150°C and +200°C.

The dielectric spectrometer used was equipped with an HP-BASIC type computer, which controls both the oven system and the spectrometer, and was able to perform a complete measurement series over a broad range of temperatures and frequencies without operator interaction. The computer also calculated the dielectric properties of the materials from the measurement results as obtained by the FRA or the LCR meter. A complete measurement series as reported here, namely a temperature scan from −150°C to +150°C with 1°C measurement intervals and dielectric measurements at frequencies between 100 mHz and 10 kHz with two measurement points per decade, took about 16 h.

Dynamic mechanical measurements in torsion at 0.2153 Hz, as a function of temperature, were performed on a torsion pendulum apparatus designed and built at DSM. Standard measurements are performed at only one, historically determined, frequency (0.2153 Hz), while the temperature can be varied between −150°C and +400°C.

Mass measurements were made with a Mettler AE240 balance, which has a resolution of 0.01 mg on a scale of 20 g.

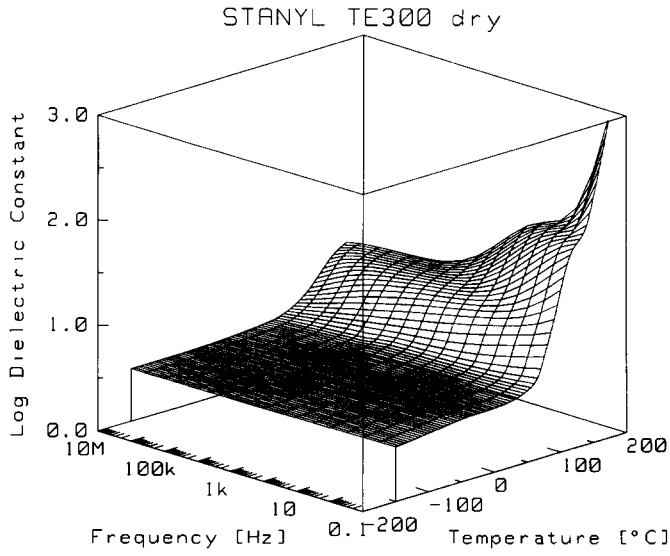

Figure 1 The dielectric constant of dry Stanyl TE300 as a function of temperature and frequency

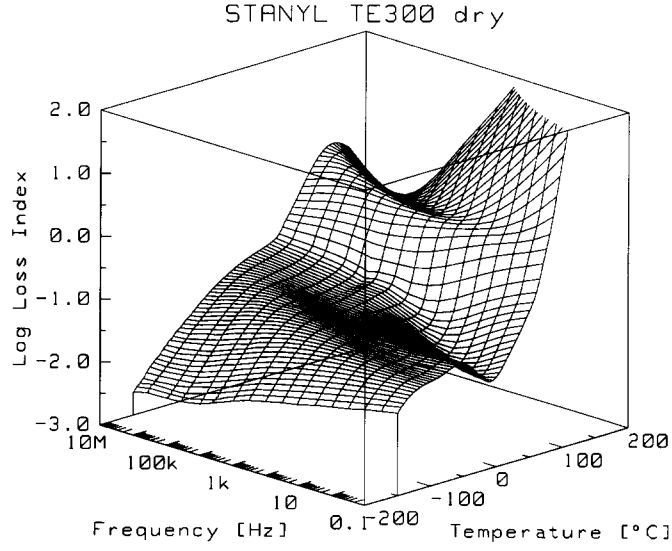

Figure 2 The dielectric loss index of dry Stanyl TE300 as a function of temperature and frequency

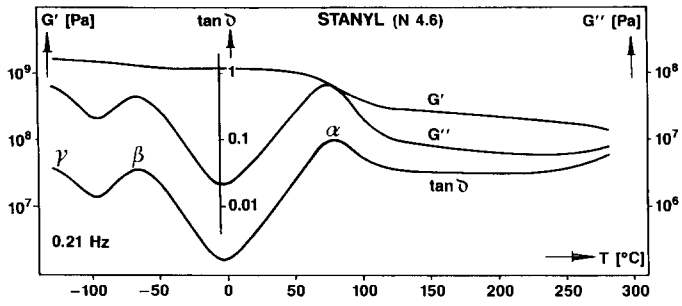

Figure 3 The mechanical storage and loss moduli, G' and G'', as a function of temperature at 0.21 Hz

RESULTS AND DISCUSSION

Dynamic dielectric and dynamic mechanical properties of dry Stanyl TE300

In *Figures 1* and *2* three-dimensional graphs of the dielectric constant ε' and the dielectric loss index ε'' of dry Stanyl TE300 are given as functions of both temperature, between −150°C and +175°C with 1°C steps, and frequency, between 100 mHz and 10 MHz, with two measurement points per decade. Note that both scales are logarithmic. The constant-temperature lines in these graphs are only shown at 5°C intervals, while the constant-frequency lines include the information for all temperatures as measured.

Figure 3 shows the results from dynamic mechanical measurements in torsion at 0.2153 Hz, as a function of temperature between −130°C and +275°C. The upper

curve shows the storage (shear) modulus G', which is plotted along the left-hand Y axis. The curve in the middle shows the loss modulus G'', which is plotted along the right-hand Y axis. The lower curve shows the mechanical loss tangent, $\tan\delta = G''/G'$, which is depicted along the axis in the middle.

Data analysis

The dielectric loss index (*Figure 2*) clearly shows three relaxation processes in the temperature interval from -150°C to $+150$°C and the onset of electrical conduction at high temperatures and low frequencies. At 0.1 Hz the loss maxima ε''_{max} are found at -125°C (γ), -65°C (β) and $+80$°C (α). Owing to the logarithmic scale, the plot of the dielectric constant (*Figure 1*) shows the γ and β polarization processes at lower temperatures only very weakly. At higher temperatures two strong relaxations are clearly visible, the first one of which correlates with the α relaxation peak as seen from the loss index. Finally, at the highest temperatures and lowest frequencies a sharp increase of the dielectric constant is seen. The loss peaks that belong to the fourth polarization process are not visible in *Figure 2* because of the high conduction losses. Using the well known mathematical approximation formula (1), one can calculate the loss index from the frequency dependence of the dielectric constant[8]:

$$\varepsilon''(\omega, T) \simeq -(\pi/2)\partial\varepsilon'(\omega, T)/\partial \ln \omega \qquad (1)$$

With this approximation formula, only the polarization losses are calculated, since pure conduction effects have no effect on the dielectric constant. The loss index calculated using relation (1) clearly shows loss peaks for the fourth relaxation process (denoted MWS, as explained later).

In the mechanical measurements, three relaxation processes are found, two at temperatures below room temperature, -130°C (γ) and -65°C (β), respectively, and one at 78°C (α). The positions of the loss maxima in G'' correlate reasonably well with the dielectric loss maxima at the lowest frequencies. The fourth dielectric relaxation process, at high temperatures, is not found in mechanical measurements.

In *Figure 4* we have constructed a so-called relaxation map for dry Stanyl TE300, which shows the frequencies

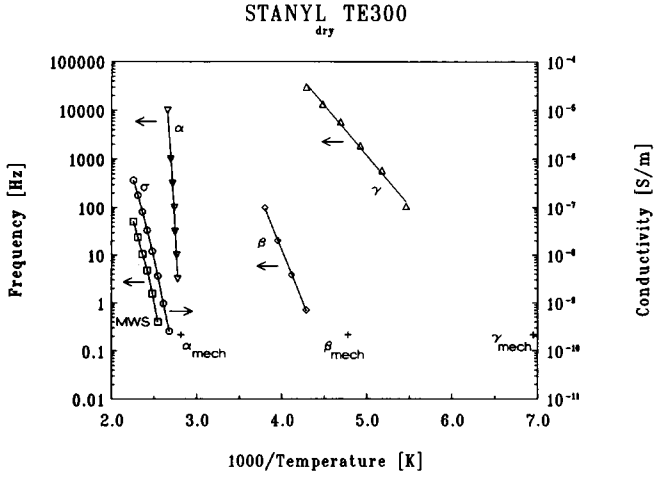

Figure 4 A relaxation map of the dry Stanyl TE300 sample. The mechanical results have been included, using the symbol (+)

of maximum dielectric loss as functions of the reciprocal temperature for the four detected relaxation processes. If possible, the frequencies of maximum dielectric loss were extracted from a constant-temperature frequency scan of the dielectric properties. For this purpose a second measurement series was performed with ten measurement frequencies per decade and 5°C temperature intervals. In *Figure 4* the mechanical relaxation maxima G''_{max} have been added using the symbol (+), although from a physical point of view a comparison with the maxima in the compliance loss should be made. In *Figure 4* we have also added the conductivity σ (S m^{-1}) of the sample as a function of the reciprocal temperature and depicted it along the right-hand axis.

The temperature dependences of the γ and β relaxations follow the Arrhenius law[1]:

$$\ln \tau(T) = \ln \tau_\infty + E_{act}/RT \qquad (2)$$

where $\tau(T)$ (s) ($=1/2\pi f_{max}$) is the retardation time of the loss process, as a function of temperature T (K), τ_∞ (s) is a constant, the retardation time at infinite temperature, E_{act} (J mol^{-1}) is the activation energy of the relaxation process and R is the gas constant (8.3144 J mol^{-1} K^{-1}).

The Arrhenius parameters E_{act} and τ_∞ of the γ and β relaxations are listed in *Table 1*. These two relaxations are similar to the glassy-state relaxations found in other polyamides[1,2]. The γ transition is usually considered to be related to a rotational motion of the chain segments, mainly CH_2 segments, between the interchain hydrogen bonds. The β transition is considered to be related to a mechanism of motion of the amide bonds and its associated water molecules. This picture is supported by a comparison of the results from the dielectric and mechanical investigations. The dielectric γ relaxation, which is due to a motion of the apolar CH_2 segments, is weak, whereas the β relaxation, which involves motion of the polar amide bonds, is much more pronounced in the dielectric measurements.

The α relaxation around 80°C, which causes a stepwise decrease in mechanical storage modulus G' and a sharp increase in dielectric constant, is thought to be due to the glass–rubber transition of the amorphous phase in the sample. In polyamide-4,6 the glass–rubber transition is found at 10–20°C higher temperatures than in other polyamides. The position of the loss maxima in the relaxation map shows WLF (Williams–Landel–Ferry) behaviour, which is characteristic of the glass transition[1]:

$$\ln \tau(T) = \ln \tau_0 - \frac{C_1(T - T_0)}{C_2 + T - T_0} \qquad (3)$$

in which $\tau(T)$ (s) is the retardation time of the loss process, as a function of temperature T (K), τ_0 (s) is the retardation time at an arbitrarily chosen reference temperature T_0 (K), and C_1 and C_2 (K) are constants, the WLF parameters. *Table 1* contains the WLF parameters that were determined from a least-squares fit for the α transition with a reference frequency of 1 Hz.

The fourth relaxation process is a liquid/rubber-state relaxation, which is only found in dielectric measurements. Owing to this relaxation, the dielectric constant increases sharply to a level of about 60, which is very high for a dipolar polarization process. Moreover, both this relaxation process and the electrical conductivity of the sample follow the Arrhenius law with a nearly equal activation energy, as is shown in *Table 1*, where the

Table 1 The Arrhenius and WLF relaxation parameters of Stanyl TE300

	γ	β	α	MWS	σ
E_{act} (kJ mol^{-1})	39.6	84.2	–	138	144
τ_∞ (s)	5.9×10^{-15}	3.3×10^{-20}	–	1.4×10^{-19}	–
σ_∞ (S m^{-1})	–	–	–	–	$4.1 \times 10^{+10}$
C_1	–	–	31.2	–	–
C_2 (K)	–	–	43.0	–	–
T_0 (K) (1 Hz)	–	–	85.2	–	–

Arrhenius parameters of the MWS relaxation and the electrical conductivity are also listed. This strongly suggests that the relaxation is due to an interfacial polarization process of the Maxwell–Wagner–Sillars (MWS) type. The electrical conductivity of the crystalline phase is much lower than the conductivity of the amorphous phase. Free charge carriers, probably ions, which move through the amorphous phase of the sample, are hindered in their motion by the crystalline phase of the material and pile up at interfaces between the amorphous and the crystalline phase. This causes the build-up of a macroscopic charge separation, or space charge, with a relatively long retardation time. Therefore, this polarization process is only found at lower frequencies and at higher temperatures, at which the material becomes conductive because of the transition to the rubber/liquid state.

The sharp increase of the low-frequency dielectric constant at the highest temperature is probably an electrode polarization (EP) effect, i.e. the formation of a boundary layer of blocked ions at the electrode surface. The measured cell capacity increases strongly because of this electrode polarization. This effect obscures the dielectric properties of the material under investigation.

A comparison between the dielectric properties of polyamide-4,6 and polyamide-6,6

Figures 5–8 show two-dimensional plots of the dielectric constant ε' and loss index ε'' of dry polyamide-4,6 Stanyl TE300 and of dry polyamide-6,6, as a function of temperature between −150°C and +150°C, as measured at 11 frequencies in the range from 100 mHz up to 10 kHz, with two measurement frequencies per decade. For the plots of the dielectric constant, both a linear and a logarithmic scale were used. The upper set of curves shows the linear data, plotted along the left-hand axis, while the lower set of curves shows the logarithmic data, plotted along the right-hand axis. The loss index was only plotted along a logarithmic axis.

The general trend in the dielectric data for both polyamides is quite similar, but a few differences are observed:

(i) The unrelaxed permittivity of polyamide-6,6, as seen from the dielectric constant at −150°C, is about 0.1–0.2 lower than the unrelaxed permittivity of polyamide-4,6, probably due to the lower density of polyamide-6.6.

(ii) The loss peaks of the β process are more intense in polyamide-4,6 than in polyamide-6,6. This is in agreement with the higher concentration of amide bonds in polyamide-4,6. A freedom of motion of these amide bonds was assumed to be the cause of this relaxation process.

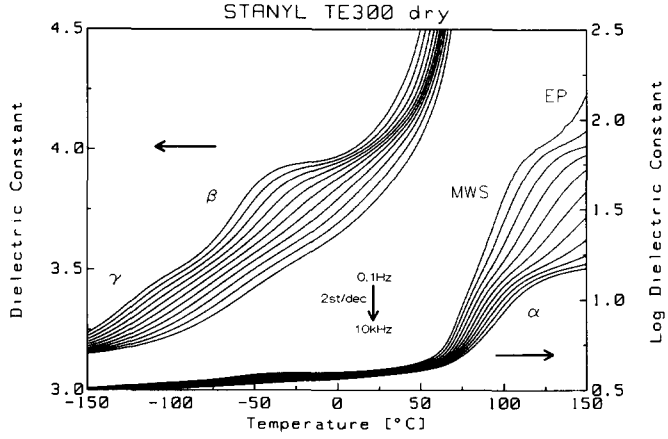

Figure 5 The dielectric constant of dry Stanyl TE300 as a function of temperature, for several frequencies

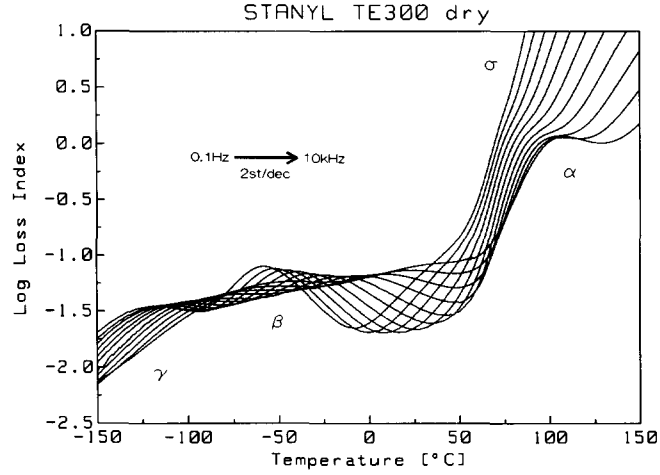

Figure 6 The dielectric loss index of dry Stanyl TE300 as a function of temperature, for several frequencies

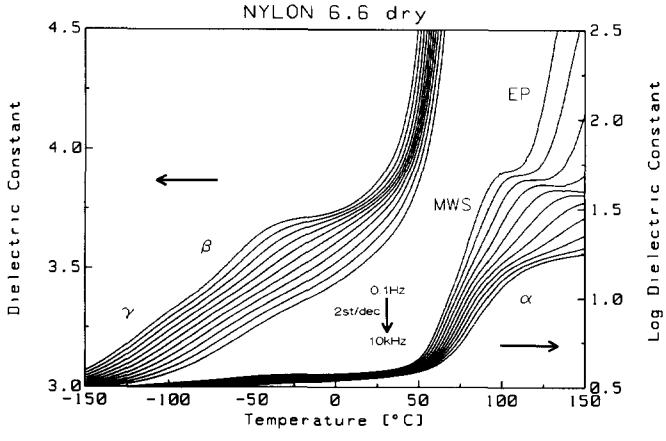

Figure 7 The dielectric constant of dry polyamide-6,6 as a function of temperature, for several frequencies

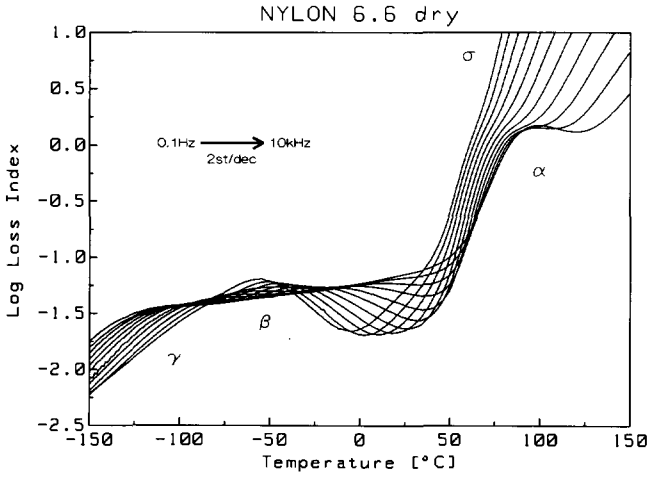

Figure 8 The dielectric loss index of dry polyamide-6,6 as a function of temperature, for several frequencies

(iii) The loss peaks of the α process in polyamide-4,6 are found at about 10°C higher temperatures than those in polyamide-6,6, indicating that the glass–rubber transition in polyamide-4,6 is shifted to about 10°C higher temperatures.

(iv) The Maxwell–Wagner–Sillars polarization is stronger in polyamide-4,6 than in polyamide-6,6, indicating a higher degree of crystallinity of polyamide-4,6, while the MWS polarization process in Stanyl is found at higher temperatures.

(v) The electrical conductivity of polyamide-6,6 is, at temperatures above its glass transition T_g, higher than the electrical conductivity of polyamide-4,6. This is due to two effects: (1) The conductivity is a function of $T - T_g$, and the T_g of polyamide-6,6 is lower than the T_g of polyamide-4,6. (2) Conduction is due to the amorphous phase, and the crystallinity of polyamide-6,6 was indicated to be lower than that of polyamide-4,6.

(vi) Electrode polarization effects are more pronounced in polyamide-6,6 because of its higher electrical conductivity.

The dielectric properties of wet Stanyl TE300

Figures 9–12 show the dielectric constant and the loss index of the 2 wt% and 4 wt% wet Stanyl TE300 samples, as functions of temperature between −150°C and +150°C, measured at 11 frequencies between 100 mHz and 10 kHz, with two measurement frequencies per decade. At temperatures above +75°C these measurements are less well defined owing to the desorption of water from the samples. Especially in the 4 wt% sample the curves at higher temperatures show a tendency to bend down, which is believed to be an artefact due to loss of water.

The wet samples still show the four relaxation processes as found in dry Stanyl. In *Figure 13* we have constructed a relaxation map for the dry and the wet samples, which will be discussed in the following.

As listed in *Table 2*, the γ process is, as a result of the water uptake, reduced in amplitude from $\log(\varepsilon''_{max}) = -1.5$ in the dry sample to $\log(\varepsilon''_{max}) = -1.85$ in the 4 wt% sample. The step in the dielectric constant at the γ relaxation also becomes smaller with increasing water content, indicating a decrease in the number of orienting dipoles or their dipole moment. The dipoles that are involved in this relaxation are probably more restricted in their motion due to increasing hydrogen bonding between the chains. The loss maxima of the γ relaxation in the wet samples are too weak for estimating their position properly. Therefore we omitted the γ relaxation in the wet samples from the relaxation map in *Figure 13*.

By contrast, the loss peaks of the β process are of the same magnitude in the dry and wet samples, but they are broadened along the temperature axis. At the same time, the step in the dielectric constant is much bigger

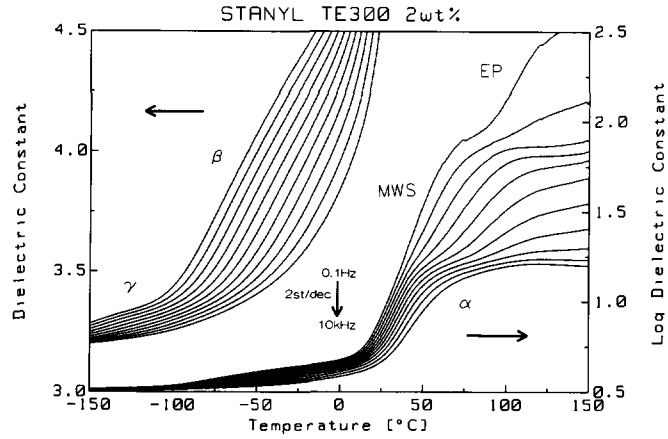

Figure 9 The dielectric constant of Stanyl TE300 after 2.4 wt% water uptake as a function of temperature, for several frequencies

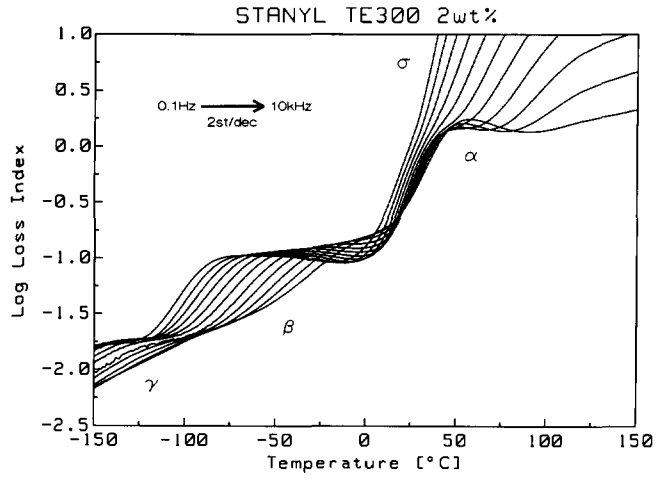

Figure 10 The dielectric loss index of Stanyl TE300 after 2.4 wt% water uptake as a function of temperature, for several frequencies

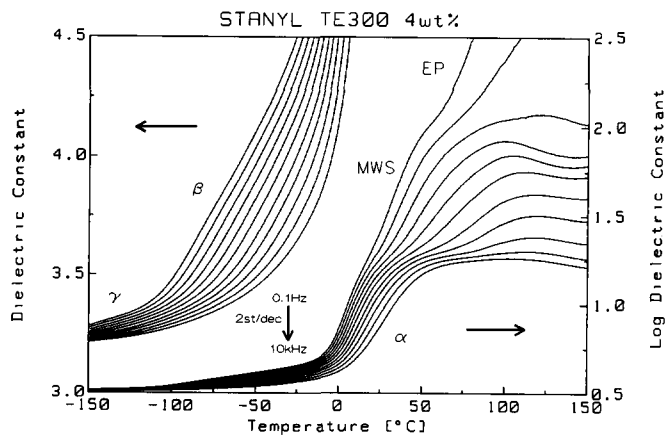

Figure 11 The dielectric constant of Stanyl TE300 after 4.3 wt% water uptake as a function of temperature, for several frequencies

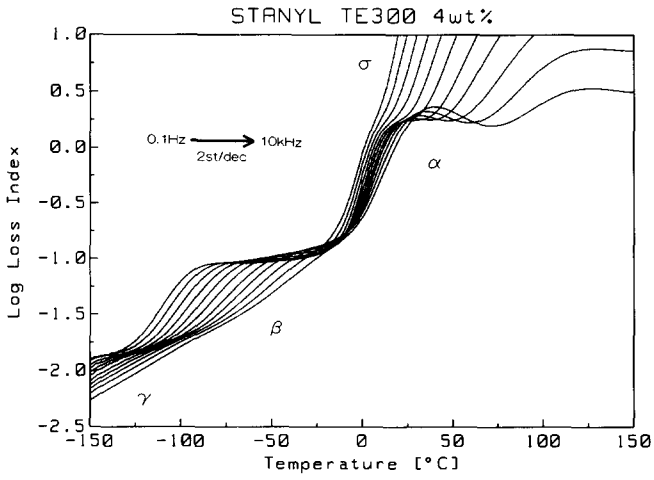

Figure 12 The dielectric loss index of Stanyl TE300 after 4.3 wt% water uptake as a function of temperature, for several frequencies

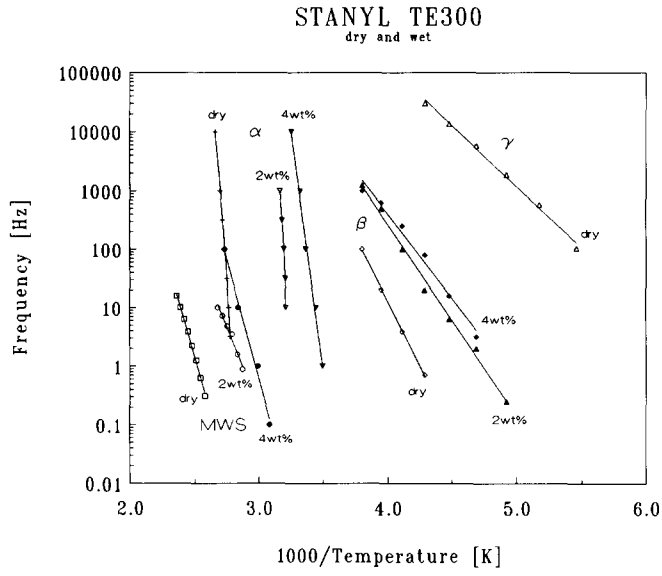

Figure 13 A relaxation map of the dry and wet Stanyl TE300 samples

Table 2 The logarithm of the maximum dielectric loss $\log(\varepsilon''_{max})$ of the loss processes in dry and wet Stanyl TE300

	γ	β	α
Dry	−1.5	−1.1	0.1
2 wt%	−1.75	−1.0	0.25
4 wt%	−1.85	−1.1	0.35

Table 3 Arrhenius parameters for the β relaxation in wet Stanyl TE300

	β (2 wt%)	β (4 wt%)
E_{act} (kJ mol^{-1})	62.6	55.1
τ_∞ (s)	5.2×10^{-17}	1.2×10^{-15}

in the wet samples than in the dry sample. This indicates that the number of orienting dipoles or their dipole moment increases with increasing water uptake. Since water molecules are bound to the polar amide groups involved in the β relaxation, an increase of the dipole moment of the amide groups due to bonded water molecules is to be expected. The Arrhenius parameters for the β relaxation are listed in *Tables 1* and *3*. It appears that the activation energy decreases with increasing water content, indicating that the potential energy barrier involved in this mechanism of motion is reduced due to the presence of absorbed water molecules. Probably the interchain hydrogen bonds between the amide bonds rotating in the β relaxation process are weakened by the presence and insertion of water molecules. Moreover, the peak broadening along the temperature axis suggests that the potential energy barriers for rotation of the amide groups are spread out over a distribution of values, indicating differences between the local environments of the amide groups through the sample.

In the case of the α relaxation, both the magnitude of the loss peaks and the step in the dielectric constant increase due to the water uptake. At the same time the relaxation loss maxima shift to lower temperatures with increasing water content. This shift of the loss peaks shows the internal plasticizing effect of the absorbed water molecules, which is well known for all polyamides. The glass transition temperature of the material is strongly influenced by the absorption of water. For dry samples the loss maximum at 1 Hz due to the glass–rubber transition is found at 85.2°C, after 2.4 wt% water uptake this loss maximum is found at 37.3°C, while after 4.3 wt% water uptake the α relaxation loss maximum is found at about 0.3°C. The variance in the parameters of the WLF fit on the wet samples strongly increases with increasing water uptake, while for the 4 wt% sample the Arrhenius equation seemed to be more appropriate. Therefore no results for the WLF parameters of the wet samples are given here.

The electrical conduction in the wet samples is enhanced as a result of both the lowering of the glass transition temperature and the absorption of polar water molecules, which may give rise to the formation of a co-continuous electrically conductive water phase. Owing to the higher conductivity the MWS relaxation is also found at lower temperatures, although its magnitude is not influenced by the water absorption.

ACKNOWLEDGEMENTS

The authors thank Mr Havenith and Mr Goertz for supplying and conditioning the samples and Mr Baetsen for performing the measurements on the samples. The authors also thank Professor Dr van Turnhout from the Delft University of Technology, The Netherlands, for fruitful discussions about the detection and interpretation of low-frequency interfacial polarization mechanisms.

REFERENCES

1 McCrum, N. G., Read, B. E. and Williams, G. 'Anelastic and Dielectric Effects in Polymeric Solids', Wiley, London, 1967
2 Hedvig, P. 'Dielectric Spectroscopy of Polymers', Adam Hilger, London, 1977
3 Baird, M. E. and Goldsworthy, G. T. *J. Polym. Sci.* (*B*) 1968, **6**, 737
4 Baird, M. E., Goldsworthy, G. T. and Creasy, C. J. *Polymer* 1971, **12**, 159
5 Gil-Zambrano, J. L. and Juhasz, C. *J. Phys.* (*D*) *Appl. Phys.* 1982, **15**, 119
6 Gaymans, R., van Utteren, T., van den Berg, J. and Schuyer, J. *J. Polym. Sci., Polym. Chem. Edn* 1977, **15**, 537
7 Roerdink, E. and Warnier, J. *Polymer* 1985, **26**, 1582
8 Böttcher, C. J. F. and Bordewijk, P. 'Theory of Electric Polarization', Elsevier, Amsterdam, 1978, Vol. II